This article has been accepted for publication in a future issue of this journal, but has not been fully edited. Content may change prior to final publication. Citation information: DOI 10.1109/LPT.2017.2700619, IEEE Photonics Technology Letters

Integrated Reconfigurable Unitary Optical Mode Converter using MMI Couplers

Rui Tang, Takuo Tanemura, *Member, IEEE*, and Yoshiaki Nakano, *Member, IEEE*

***Abstract*—Reconfigurable unitary optical mode converters that can convert multiple orthogonal spatial modes into different orthogonal modes without fundamental optical loss are important for mode-division-multiplexed (MDM) optical communication, imaging, and quantum computation. In this paper, we propose a novel integrated reconfigurable unitary optical mode converter, which consists of cascaded multimode interference (MMI) couplers and phase shifter arrays. We numerically investigate its ability to realize arbitrary unitary mode conversion and demonstrate its applicability to mode unscrambling as well as mode switching in MDM transmission systems.**

***Index Terms*—Optical mode converter, MMI coupler, Mode unscrambling.**

I. Introduction

Optical spatial mode converters are receiving growing attention in the field of mode-division-multiplexed (MDM) optical communication, imaging, and quantum computation [1-6]. While all linear optical devices can be viewed as optical mode converters in general [7], it is possible to simultaneously convert multiple orthogonal spatial modes into different orthogonal modes without fundamental optical loss by using a unitary mode converter [8]. For example, a free-space unitary optical mode converter based on multi-plane light conversion has been demonstrated to achieve nearly loss-less multiple-input-multiple-output (MIMO) mode multiplexing [9] and applied in several MDM optical transmission experiments [10-11].

For many applications, including adaptive optical MIMO (de)multiplexing and high-speed mode switching in MDM networks, it is important to realize unitary mode converters that are reconfigurable. To this end, various approaches have been demonstrated by using spatial light modulators (SLMs) [12-13]. While excellent performance with low crosstalk has been demonstrated, integrated devices are preferable due to the compactness, lower cost, and higher stability, when employed in practical systems [14]. Recently, integrated reconfigurable unitary mode converters based on cascades of 2 × 2 Mach-Zehnder interferometers (MZI) and phase shifters has been proposed [15] and experimentally demonstrated on Si and InP [16-20]. Demonstrated applications using this structure include unscrambling coupled modes occurred in multimode fibers [16-18], as well as photonic boson sampling on chip [20]. Although the configuration of phase shifters for a desired unitary conversion is relatively straightforward in this structure, the unitarity may be disturbed when it comes to large-scale mode conversion because each path has different coupling loss. Adding a corresponding symmetry counterpart can solve this problem [15], but requires approximately double footprint and power consumption.

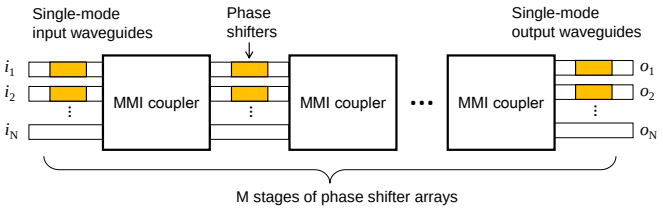

Fig. 1. Schematic structure of the proposed integrated reconfigurable unitary optical mode converter.

In this paper, we propose a novel integrated reconfigurable $N \times N$ unitary optical mode converter using cascaded $N \times N$ multimode interference (MMI) couplers and phase shifter arrays. We numerically investigate its ability to realize arbitrary unitary mode conversion and demonstrate its applicability to mode unscrambling as well as mode switching in MDM transmission systems. Owing to relatively simple symmetrical geometry and use of robust MMI couplers, the proposed scheme is expected to realize smaller path-dependent insertion loss and footprint when fabricated on low-index-contrast photonic integrated platforms such as InP and silica.

II. Structure and Operating Principle

The schematic structure of the proposed device is shown in Fig. 1, which consists of series of $N \times N$ MMI couplers and phase shifter arrays. The $N \times N$ transfer matrix $\mathbf{T}$, which describes the coupling from the complex amplitudes at N input single-mode waveguides into those at N output single-mode waveguides, is expressed as

$$\mathbf{T} = \mathbf{\Phi}_M \cdot \mathbf{M} \cdot \mathbf{\Phi}_{M-1} \cdots \mathbf{M} \cdot \mathbf{\Phi}_1, \qquad (1)$$

where $\mathbf{M}$ and $\mathbf{\Phi}_i$ are the transfer matrices of MMI couplers and

Manuscript received XXXX, 2016; revised XXXX, 201X; accepted XXXX, 201X. This work was financially supported by the Grant-in-Aid of Japan Society for the Promotion of Science #26000010.

The authors are with the Department of Electrical Engineering and Information Systems, Graduate School of Engineering, The University of Tokyo, Bunkyo-ku, Tokyo 113-8656, Japan (e-mail: rui.tang@hotaka.t.u-tokyo.ac.jp; tanemura@ee.t.u-tokyo.ac.jp; nakano@ee.t.u-tokyo.ac.jp).

Color versions of one or more of the figures in this letter are available online at http://ieeexplore.ieee.org.

Digital Object Identifier XX.XXXX/XXXXXXXXXXX

This article has been accepted for publication in a future issue of this journal, but has not been fully edited. Content may change prior to final publication. Citation information: DOI 10.1109/LPT.2017.2700619, IEEE Photonics Technology Letters

the *i*-th stage phase shifter array, respectively, and *M* is the total number of phase shifter stages. $\mathbf{\Phi}_i$ is a unitary matrix with only diagonal elements; **M** is also a unitary matrix when neglecting the path-dependent coupling loss [21]. Similar to the multi-plane light conversion scheme demonstrated in free space [9], which represents a special case with **M** expressing the Fourier transform, it can be proved from the group theory [12, 22] that an arbitrary unitary mode conversion can be realized by using sufficient number of MMI coupler stages and configuring the phase shifters appropriately. To realize $N \times N$ mode conversion, the number of stages *M* should be no less than *N* when considering the necessary degrees of freedom. The precise condition for required number of *M*, on the other hand, depends on the required accuracy and extinction ratio that need to be achieved in actual applications.

Compared with the previous scheme based on cascaded 2 × 2 MZI couplers [15], our scheme has a drawback that it requires an iterative calculation to derive the optimal phase shifter conditions, which may limit some applications. Once the condition is found, however, we may repeat the iterative optimization process over time by monitoring the crosstalk to track the evolution of the target transfer matrix caused by slow environmental changes, such as temperature drift and slight movement of optical fibers. On the other hand, the use of MMI coupler as the building block may provide unique advantage of our scheme. It has been generally recognized that MMI couplers are robust against fabrication errors [23, 24] and can be scaled to large number of ports with relatively small footprint [25]. These features are especially salient for InP platform, and have been utilized in realizing recent commercial InP coherent receivers [26]. Finally, the symmetrical architecture of our device may also be advantageous in reducing the path-dependent insertion loss without the need of adding symmetrical counterpart [15].

III. Numerical Analysis

Numerical simulations were carried out to verify the validity of this scheme and to derive necessary number of stages *M* to perform $N \times N$ unitary conversions with sufficient accuracy. For simplicity, we assumed ideal MMI couplers in this work and used the unitary matrix **M** as described in [21] to calculate Eq. (1). While more rigorous simulations are required to study fabrication tolerance of the real device, the simplified ideal MMI model has been proved to be valid in designing large-scale couplers [25] and should be adequate in verifying the basic concept of the scheme. For a given desired unitary matrix, we used the simulated annealing method [12] to derive the required phase shift at each phase shifter. The mean square error (MSE) was then used to evaluate the difference between the generated $N \times N$ transfer matrix $\mathbf{T}'$ and the desired matrix **T:**

$$MSE = \frac{1}{N^2}\sum_{i=1,j=1}^{N,N}\left|T'_{ij} - T_{ij}\right|^2, \qquad (2)$$

where *i* (*j*) is the row (column) number of $\mathbf{T}'$ and **T**. Using MSE as the cost function, we repeated the simulated annealing algorithm for 5 different random unitary matrices as **T** with 5 different initial conditions (total of 25 conditions for each case).

The random unitary matrix **T** was generated by first preparing a random Hermitian matrix $\mathbf{H} = (\mathbf{A} + \mathbf{A}^{\dagger})/2$, where **A** is a $N \times N$ matrix with N^2 random complex values, and then converting it to a unitary matrix by $\mathbf{T} = \exp(i\mathbf{H})$. The initial conditions were also generated randomly by setting the phase shift at each phase shifter to a random value between 0 and 2π. The

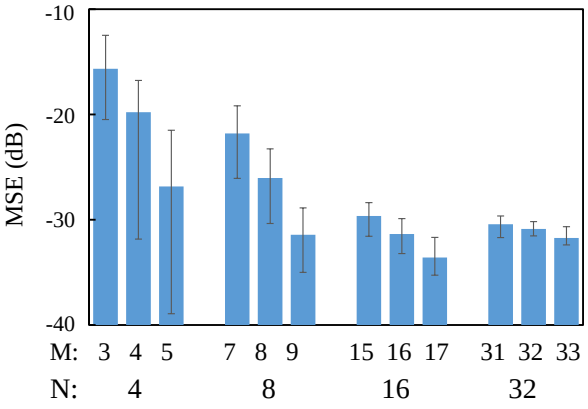

Fig. 2. MSE of optimally tuned unitary converter for 25 different conditions with varying *N* and *M*.

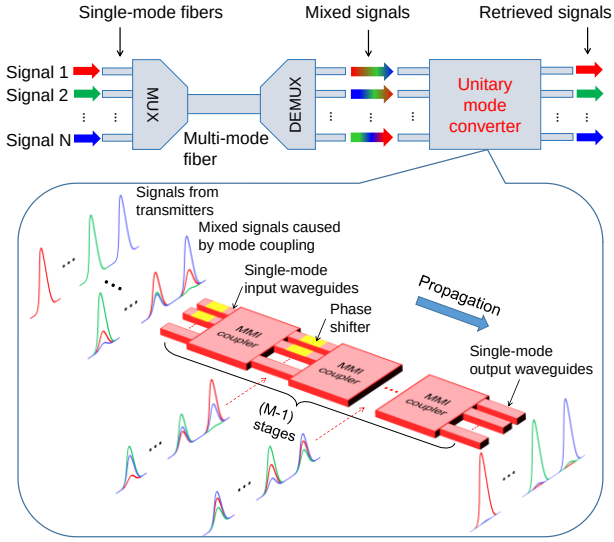

Fig. 3. Schematic diagram of applying the proposed unitary mode converter to unscramble mixed signals in MDM system.

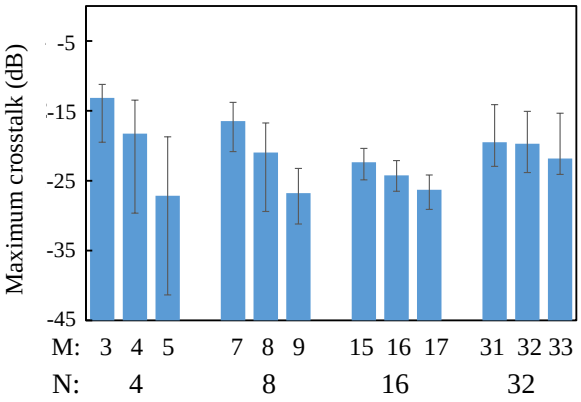

Fig. 4. Calculated results of maximum crosstalk between spatial channels after mode unscrambling.

This article has been accepted for publication in a future issue of this journal, but has not been fully edited. Content may change prior to final publication. Citation information: DOI 10.1109/LPT.2017.2700619, IEEE Photonics Technology Letters

resolution of phase control was set to 0.01 rad to reflect realistic cases.

Figure 2 shows the MSE of the unitary mode converter with various values of N and M after deriving the optimal phase shifter condition by the simulated annealing method [12]. The error bar shows the variation of 25 different conditions used in each case. We see that the MSE decreases with increased number of stages, because the errors in phase control can be gradually compensated for by the increased degrees of freedom. More specifically, when $M > N$, MSE is reduced below -20 dB for all cases.

Next, we analyze the performance of this device when it is applied to mode unscrambling in MDM transmission system as shown in Fig. 3. Let us represent the mode coupling matrix by $\mathbf{U}$, which includes all the linear mode-coupling effects that may occur inside the mode multiplexer/demultiplexer as well as during the transmission inside a multimode fiber. The original signals can then be retrieved by applying the inverse matrix $\mathbf{U}^{-1}$. If the mode-dependent loss (MDL) of the entire system is negligible, $\mathbf{U}^{-1}$ is a unitary matrix, which can be directly generated by the unitary optical mode converter. Even in a more general and realistic case where MDL is non-negligible, $\mathbf{U}^{-1}$ can still be factorized into a product of two unitary matrices and one diagonal matrix through singular value decomposition [7, 27], which can be realized by the combination of two unitary mode converters and one amplitude modulator array [28].

For simplicity, here we consider the case where MDL is negligible, so that single unitary optical mode converter can be used to unscramble the modes as illustrated in Fig. 3. Note that the phase shifter array after the final MMI coupler is omitted in Fig. 3 since the absolute optical phase at each output port is insignificant for mode-scrambling application. As a result, we only need M-1 stages of phase shifters. Assuming that the mode coupling inside an optical fiber occurs randomly in the transmission line [29], we generate random unitary matrix $\mathbf{U}$ by the same method that we used in deriving Fig. 2. To evaluate the device performance quantitatively, we examine the off-diagonal elements of $\mathbf{T}' \cdot \mathbf{U}$ [where $\mathbf{T}'$ is the actual generated matrix as defined in Eq. (2)], which represent the crosstalk between different spatial channels after mode unscrambling; if the device is perfect, $\mathbf{T}' = \mathbf{U}^{-1}$ so that off-diagonal elements of $\mathbf{T}' \cdot \mathbf{U}$ are zero. We define the maximum crosstalk of the device as the largest absolute square of the off-diagonal elements.

Figure 4 shows the maximum crosstalk after mode unscrambling, calculated for the $N \times N$ unitary matrices $\mathbf{T}$ that we derived in Fig. 2. We can see that the crosstalk decreases with increased number of stages M, which is consistent with the dependence of MSE shown in Fig. 2. For example, when N = 16 and M = 16, the crosstalk is below -24 dB. Figure 5(a) and 5(b) plot the absolute square of all 16 × 16 elements of $\mathbf{U}$ and $\mathbf{T}' \cdot \mathbf{U}$, respectively, in an example case with N = 16 and M = 16. While $\mathbf{U}$ has significant level of off-diagonal components [Fig. 5(a)], corresponding to large modal mixing at the input of the device, off-diagonal components are suppressed for $\mathbf{T}' \cdot \mathbf{U}$ [Fig. 5(b)], demonstrating that the modes are unscrambled

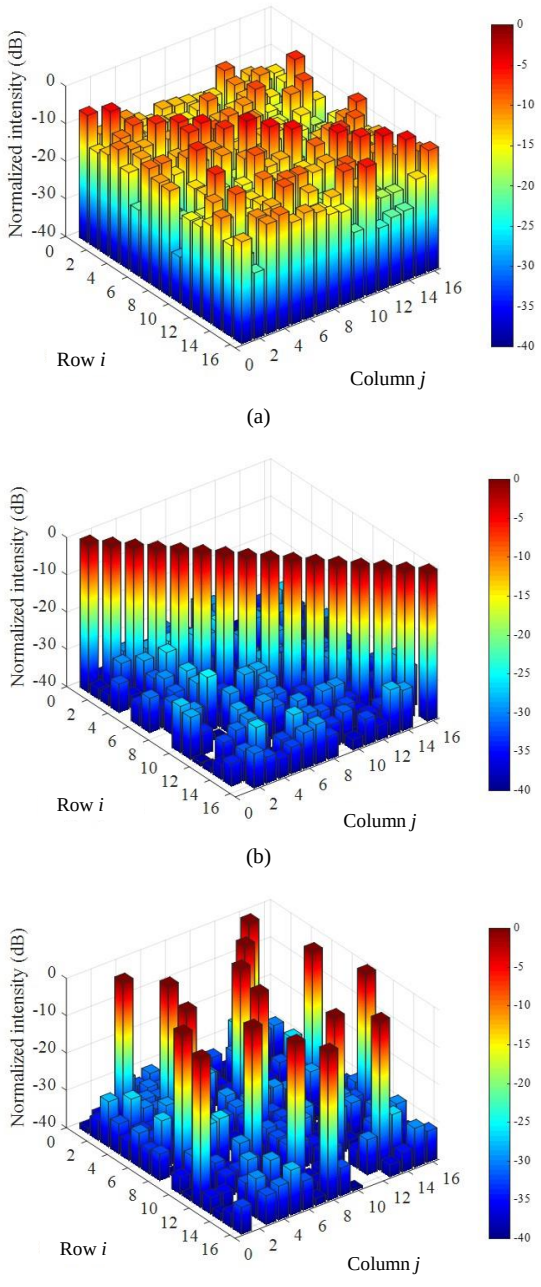

Fig. 5. Normalized intensity (absolute square) of 16 × 16 matrix components of (a) $\mathbf{U}$ (device input), (b) $\mathbf{T}' \cdot \mathbf{U}$ (device output), and (c) $\mathbf{T}' \cdot \mathbf{U}$ (device output with switching-associated mode unscrambling). N = 16, M = 16.

effectively by the device.

In addition to simple mode unscrambling, we could also transfer the input mode to another mode at the output to realize mode switching [2]. Such function can be realized by assigning the target matrix as $\mathbf{T} = \mathbf{V} \cdot \mathbf{U}^{-1}$ instead of $\mathbf{U}^{-1}$, where $\mathbf{V}$ is a permutation matrix representing the switching between desired modes. Figure 5(c) shows the absolute square of $\mathbf{T}' \cdot \mathbf{U}$ in such a case for N = 16 and M = 16. We see that the input signals are unscrambled and then switched to a different channel at the output. These results imply the applicability of the proposed device to flexible large-scale mode-switchable optical networks

This article has been accepted for publication in a future issue of this journal, but has not been fully edited. Content may change prior to final publication. Citation information: DOI 10.1109/LPT.2017.2700619, IEEE Photonics Technology Letters

[30].

IV. Conclusion

We have proposed a novel integrated reconfigurable unitary optical mode converter using cascaded MMI couplers and phase shifter arrays. We numerically demonstrated the ability of this device to implement reconfigurable $N \times N$ unitary conversion. By using more than N stages ($M > N$), desired unitary matrix was generated with MSE smaller than -20 dB for all tested cases. Moreover, we showed an example of applying the device to mode unscrambling in MDM transmission systems with up to 16 modes and a modal crosstalk less than -24 dB. We have also demonstrated its applicability to flexible mode-switching devices. With relatively simple symmetrical layout and use of robust MMI couplers, the proposed scheme is expected to be useful in reducing the path-dependent loss and footprint of reconfigurable unitary optical converter in various photonic integration platforms.

References

[1] J. Dong and K. S. Chiang, "Temperature-insensitive mode converters with CO_2-laser written long-period fiber gratings," *IEEE Photon. Technol. Lett.*, vol. 27, pp. 1006-1009, 2015.

[2] R. Takakura, M. Jizodo, A. Fujino et al., "Proposal of optical mode switch," *Jpn. J. Appl. Phys.*, vol. 53, 08MB10, 2014.

[3] Y. Huang, G. Xu, and S. T. Ho, "An ultracompact optical mode order converter," *IEEE Photon. Technol. Lett.*, vol. 18, pp. 2281-2283, 2006.

[4] S. Cai, S. Yu, M. Lan et al., "Broadband mode converter based on photonic crystal fiber," *IEEE Photon. Technol. Lett.*, vol. 27, pp. 474-477, 2006.

[5] G. Chen and J. U. Kang, "Waveguide mode converter based on two-dimensional photonic crystals," *Opt. Lett.*, vol. 30, pp. 1656-1658, 2005.

[6] A. L. Y. Low, Y. S. Yong, A. H. You et al., "A five-order mode converter for multimode waveguide," *IEEE Photon. Technol. Lett.*, vol. 16, pp. 1673-1675, 2004.

[7] D. A. B. Miller, "All linear optical devices are mode converters," *Opt. Express*, vol. 20, pp. 23985-23993, 2012.

[8] D. A. B. Miller, "Self-configuring universal linear optical component," Photon. Res. vol. 1, pp. 1-15, 2013.

[9] G. Labroille, B. Denolle, P. Jian et al., "Efficient and mode selective spatial mode multiplexer based on multi-plane light conversion," *Opt. Express*, vol. 22, pp. 155990-15607, 2014.

[10] K. Igarashi, D. Souma, Y. Wakayama et al., "114 space-division-multiplexed transmission over 9.8-km weakly-coupled-6-mode uncoupled-19-core fibers," in *Proc.* OFC, 2015, paper Th5C.4.

[11] C. Simonneau, A. D'amato, P. Jian et al., "4×50Gb/s transmission over 4.4 km of multimode OM2 fiber with direct detection using mode group multiplexing," in *Proc.* OFC, 2016, paper Tu2J.3.

[12] J. F. Morizur, L. Nicholls, P. Jian et al., "Programmable unitary spatial mode manipulation," *J. Opt. Soc. Am. A*, vol. 27, pp. 2524-2531, 2010.

[13] J. Carpenter, B. J. Eggleton, and J. Schröder, "110x110 optical mode transfer matrix inversion," *Opt. Express*, vol. 22, pp. 96-101, 2014.

[14] C. R. Doerr, "Proposed architecture for MIMO optical demultiplexing using photonic integration," *IEEE Photon. Technol. Lett.*, vol. 23, pp. 1573-1575, 2011.

[15] D. A. B. Miller, "Reconfigurable add-drop multiplexer for spatial modes," *Opt. Express*, vol. 21, pp. 20220-20229, 2013.

[16] F. Morichetti, A. Annoni, S. Grillanda et al., "4-channel all-optical MIMO demultiplexing on a silicon chip," in *Proc.* OFC, 2016, paper Th3E.7.

[17] D. Melati, A. Alippi, and A. Melloni, "Reconfigurable photonic integrated mode (de)multiplexer for SDM fiber transmission," *Opt. Express*, vol. 24, pp. 12625-12634, 2016.

[18] D. Melati, A. Alippi, A. Annoni et al., "Integrated all-optical MIMO demultiplexer for mode- and wavelength-division-multiplexed transmission," *Opt. Lett.*, vol 42, pp. 342-345, 2017.

[19] A. Ribeiro, A. Ruocco, L. Vanacker et al., "Demonstration of a 4 ×4-port universal linear circuit," Optica, vol. 3, pp. 1348-1357, 2016.

[20] N. C. Harris, D. Bunandar, M. Pant et al., "Large-scale quantum photonic circuits in silicon," *Nanophotonics*, vol. 5, pp. 456-468, 2016.

[21] M. Bachmann, P. A. Besse, and H. Melchior, "General self-imaging properties in N × N multimode interference couplers including phase relations," *Appl. Opt.*, vol. 33, pp. 3905-3911, 1994.

[22] Z. I. Borevich and S. L. Krupetskii, "Subgroups of the unitary group that contain the group of diagonal matrices," *J. Math. Sci.*, vol. 17, pp. 1951-1959, 1981.

[23] P. A. Besse, M. Bachman, H. Melchior et al., "Optical bandwidth and fabrication tolerances of multimode interference couplers," *J. Lightwave Technol.*, vol. 12, pp. 1004-1009, 1994.

[24] P. E. Morrissey, H. Yang, R. N. Sheehan et al., "Design and fabrication tolerance analysis of multimode interference couplers," *Opt. Commun.*, vol. 340, pp. 26-32, 2015.

[25] T. Rasmussen, J. K. Rasmussen, and J. H. Povlsen, "Design and performance evaluation of 1-by-64 multimode interference power splitter for optical communications," *J. Lightwave Technol.*, vol. 13, pp. 2069-2074, 1995.

[26] S. Farwell, P. Aivaliotis, Y. Qian, et al., "InP coherent receiver chip with high performance and manufacturability for CFP2 modules," in *Proc.* OFC, 2014, Paper W1I.6.

[27] K. P. Ho and J. M. Kahn, "Mode-dependent loss and gain: statistics and effect on mode-division multiplexing," *Opt. Express*, vol. 19, pp. 16612-16635, 2011.

[28] Y. Shen, N. C. Harris, S. Skirlo et al., "Deep learning with coherent nanophotonic circuits," *arXiv*: 1610.02365, 2016.

[29] S. O. Arik, J. M. Kahn, and K. P. Ho, "MIMO signal processing for mode-division multiplexing: an overview of channel models and signal processing architectures," *IEEE Signal Process. Mag.*, vol. 31, pp. 25-34, 2014.

[30] N. P. Diamantopoulos, M. Hayashi, Y. Yoshida et al., "Mode-selective optical packet switching in mode-division multiplexing networks," *Opt. Express*, vol. 23, pp. 23660-23666, 2015.